Neutron dosimetry and shielding verification in commissioning of Compact Proton Therapy Centers (CPTC) using MCNP6.2 Monte Carlo code

Gonzalo F. Garcia-Fernandez, Eduardo Gallego, Jose M. Gomez-Ros, Hector R. Vega-Carrillo, Roberto Garcia-Baonza, Lenin E. Cevallos-Robalino, Karen A. Guzman-Garcia

Neutron dosimetry and shielding verification in Commissioning of Compact Proton Therapy Centers (CPTC) using MCNP6.2 Monte Carlo code

Gonzalo F. García-Fernandez[1,2*], Eduardo Gallego[1], José Mª Gómez-Ros[3], Héctor R. Vega-Carrillo[4], Lenin E. Cevallos-Robalino[1,5], Roberto García-Baonza[1], Karen A. Guzman-García[4,6]

[1]Departamento de Ingeniería Energética, ETSI Industriales, Universidad Politécnica de Madrid
José Gutiérrez Abascal 2, 28006, Madrid, Spain.

[2]Biología y Técnica de la Radiación, S.L. (Bioterra, S.L.)
Camino de los Perdigones 2, 28224, Pozuelo de Alarcón, Madrid, Spain.

[3]Centro de Investigaciones Energéticas, Medioambientales y Tecnológicas (CIEMAT)
Avda Complutense 22, 28040 Madrid, Spain.

[4]Unidad Académica de Estudios Nucleares, Universidad Autónoma de Zacatecas.
C. Ciprés, 10, 98060 Zacatecas, Zac., México.

[5]Grupo de Investigación en Sistemas de Control y Robótica, GISCOR, Universidad Politécnica Salesiana
C. Robles 107 Chambers, 090108, Guayas, Guayaquil, Ecuador.
[6]AORTech, Reserch Department, C. Purisima 227, 98085, Zacatecas, Mexico

[*]Email: gf.garcia@upm.es

Author for correspondence is:

Msc. Gonzalo García
Doctoral student - UPM
C. José Gutiérrez Abascal, 2,
28006, Madrid
Spain

E-mail: gf.garcia@upm.es

ABSTRACT

Proton therapy (PT), a type of external radiotherapy using proton beams with energies between 50 and 230 MeV, has relevant clinical advantages in some cancer treatments and consequently the growth of new Proton Centers (PTC) around the world is remarkable. Compact Proton Therapy Centers (CPTC) usually comprise one treatment room, incorporating latest technological advances in radiotherapy, and stand for the answer of vendors to the growing demand of facilities taking up small spaces. There is a huge production of stray radiation in the interaction of protons used in therapy therefore optimal design of shielding and verifications must be carried out in commissioning phases. Currently, almost 50 CPTC are under construction in several countries and consequently the study of methodologies of shielding is a prevailing task. PT is coming to Spain with two compact centers in the final stages of testing.

The aim of this work was to characterize the effectiveness of shielding in CPTC by calculating the ambient dose equivalent, H*(10), due to secondary neutrons, outside the bunker, through the Monte Carlo code MCNP6. The facility modelled was a CPTC similar to the planned for the year 2019 in Spain, made up of a superconducting synchrocyclotron proton accelerator and one treatment room with a 220º compact rotating gantry, using pencil beam scanning (PBS) as dose delivery system. Several models of the radiation sources and materials of walls were simulated, starting from a conservative assumption, followed by more realistic models with results always under the legal limits. This work is included in the project *Contributions to Shielding and Dosimetry of Neutrons in CPTC*.

Keywords: Compact proton therapy centers; Shielding commissioning; Ambient dose equivalent; MCNP6.2

1. - INTRODUCTION

The advantages of proton therapy (PT) in some cancer treatments, improving the dose conformation over the treated volume, lowering entrance dose and, in practical terms, no exit dose beyond the tumor, diminishing drastically unnecessary dose in healthy tissues, have led to a meaningful expansion of proton therapy centers (PTC) all around the world [Mohan and Grosshans, 2017]. In the last ten years the number of PTC has gone from approximately twenty facilities in 2008 to almost one hundred at the time of writing, multiplied practically by five [PTCOG, 2019]. The current trends in medical PTC is to build small compact and standard facilities, along with the renovation of the former multiple room centers (MPTC) [Schneider *et al.*, 2017]. Compact Proton Therapy Centers (CPTC) are usually equipped with a single treatment room and are characterized by being standardized and having the most advanced technology to reduce the size and footprint of the facilities [Owen *et al.*, 2016]. The first PT in Spain is expected to be operational in 2019, while the second in 2020, both of CPTC type. According to Spanish laws in radiation protection, these centers are radioactive facilities of second category, Type III, and the shielding must be designed, executed and verified following the requirements of the regulatory authority [García-Fernández *et al.*, 2019].

In PTC the protons produced for clinical uses interact with the accelerator, elements of the beam transport and patients, yielding a complex stray radiation of mixed fields composed by energetic neutrons, photons and charged particles. Neutrons produced by interaction with patient are usually named internal whereas those produced by interaction with mechanical elements are named external [Han *et al.*, 2017]. The effects induced by this secondary radiation in PTC were summarized in a classic paper as follow [Agosteo *et al.*, 1998]: 1) Unwanted dose in the treatment room (secondary dose in patients, considering protons as primary); 2) Ambient dose outside the treatment room involving exposure to professionals and general public (design and calculation of biological shielding and control of the ambient dose equivalent); 3) Activation in the enclosures and also the equipment inside the facility; 4) Air activation and neutron skyshine in the air of the facility; 5) Activation of the water of auxiliary circuits and water table in the subsoil of the enclosure; 6) Management of radioactive materials and activated waste generated in the operation.

The present research is framed inside the project *Contributions to Shielding and Dosimetry of Neutrons in CPTC*, which involves the development of methodologies to analyze the shielding efficiency and to evaluate the dose to staff and the general public in these facilities therefore is focused on the second item of the aforementioned.

The usual procedure for shielding design and calculation would cover the review of source term, set legal limits and design the walls. According to published works, the methodology followed on shielding calculations in proton therapy facilities could be summarized in three approaches [Ipe, 2010]: 1) Analytical method, where the dose at the point of interest is estimated using analytical methods, such us the Point-Source line-of-sight model or Kernel Point, collected in international guidelines as [NCRP 2005] or [IAEA 1988], for example the work of [Makita *et al.*, 2004]; 2) Monte Carlo methods, where primary and secondary particles are tracked and also interactions, taking in account the nuclear data and libraries (cross sections) and materials properties (density, compositions) [Urban and Kluson, 2012], [Prusator *et al.*, 2017]; 3) Intermediate approach, a mix of both, where analytical methods with data obtained by Monte Carlo techniques are used to verify the design [Avery *et al.*, 2008]. Nonetheless, the process involves many assumptions, always on the conservative side, therefore shielding must be verified at the commissioning stage of each center [Jägerhofer *et al.*, 2017].

The aim of this work was to characterize the effectiveness of the shielding and estimate the neutron dose by calculating the ambient equivalent dose by neutrons, H*(10), outside the bunker of an CPTC similar to the standard version of center planned for 2019 in Spain. The verification of the shielding was carried out through a stochastic approach by means of the general-purpose Monte Carlo (MC) code MCNP6® version 6.2, computing the fluences of secondary neutrons produced by interaction of the beam of protons in different points of the facility. Several models of the radiation sources were simulated, starting from conservative hypothesis considering the main sources of radiation, followed by more realistic models with data published. Different enclosure materials were also tested, carrying out different assumptions with both, conventional Portland concrete and low activation concrete. The results will be compared with experimental measurements carried out during the final commissioning stage of facility.

2. - MATERIALS AND METHODS

2.1. – Commissioning requirements and shielding verification

The advent of proton therapy to Spain is a fact with two centers in the final stage of commissioning, compact size both. The first one, planned for 2019, has a cyclotron accelerator with extraction energy at 230 MeV and a footprint close to 360 m^2 [IBA, 2019]. The second one, planned for 2020, has a synchrotron accelerator, with extraction energy adjustable between 70 and 230 MeV and a footprint near 800 m^2 [Hitachi, 2019]. In agreement with national regulations for medical accelerators, the owner of the facility, among others, shall certify that shielding has been executed in compliance with the design in the initial request, submit results of the shielding checks and tests with certificate of materials used in the building and calculus (including density and composition), and the systems planned to detect and control the radiation with the facility running. The final goal is to justify that shielding of the CPTC verifies the dose limits of 1 mSv/year for general public (outside), and 50 mSv/year (inside) for exposed workers and staff, following the optimization ALARA criteria [García-Fernández *et al.*, 2019].

The CPTC considered in this work is the standard version of the center planned for the year 2019 in Spain, composed by three main elements: firstly, the accelerator, which is a superconductor synchrocyclotron (S2C2) and is located in a separate enclosure called accelerator room (AR), secondly the beamline (BL), and finally the treatment room (GTR), with a compact rotating gantry of 220º, using pencil beam scanning (PBS) as dose delivery system to the patient [IBA, 2019].

2.2. - Modeling CPTC with MCNP6.2

Calculation and hypothesis are based in data and information published in research works. The process to validate the shielding with the MC code MCNP6® version 6.2. [Werner, 2017], [Werner *et al.*, 2018], was developed in three main stages [Ferraro and Brizuela, 2015]: 1) Defining geometry, equipment and radiation sources; 2) Modelling sources through a condensation process; 3) Shielding verification by estimating the ambient dose equivalent, H*(10), at the points of interest (behind the enclosures of the CPTC).

2.2.1 Building design, equipment and materials. From a constructive and architectural point of view, the standard CPTC modelled is a rectangle with approximate dimensions of 28 x 13 m^2 (360 m^2) and three main spaces, the accelerator room (AR), the treatment room with a compact rotating gantry (GTR) and the accessing labyrinth to the facility (Maze). On the east side there is a treatment control room (TCR) to manage the facility, besides the access to the AR is through a second maze, to reduce the stray radiation towards GTR. The free height is 3.8 m in the AR vault, 7.7 m in the GTR vault, and 3 m in the maze. Height of GTR allow the rotation of gantry, fixed to the south wall, around the isocenter, that is, the point of intersection between the proton beam in the nozzle, and the gantry axis of rotation. Lay-out and elevation of the CPTC are shown in Figure 1.

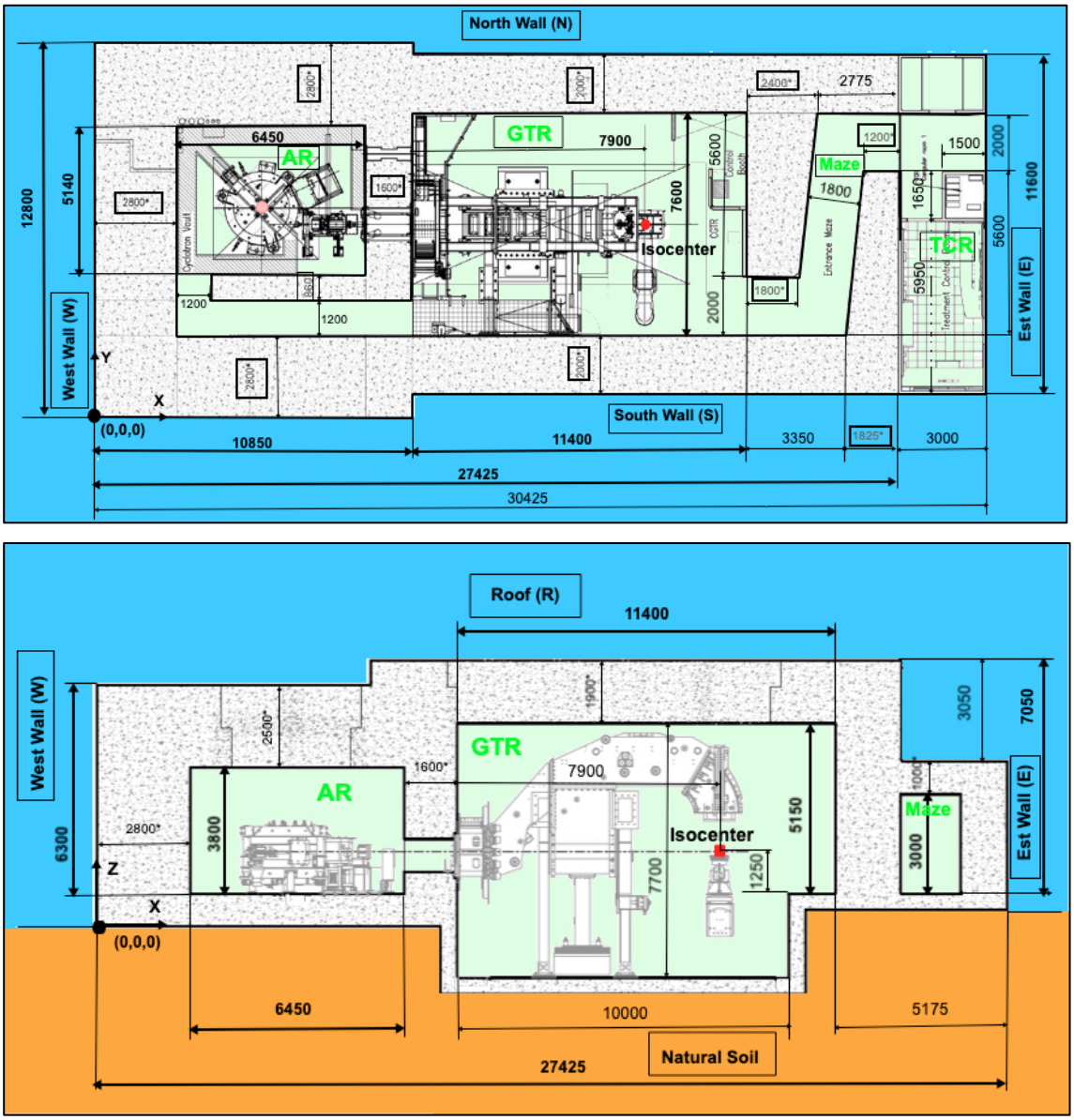

Figure 1.- CPTC layout and elevation, adapted from [Tesse, 2019] and [Stichelbaut *et al.*, 2014]

Features of main materials employed in MCNP6 are collected in Table 1. From the point of view of the materials of enclosures with influence in the shielding (walls and roofs), two different types of concrete were tested, regular concrete (2.2 g/cm^3) and low activation concrete (2.18 g/cm^3). The materials of removable hatches and hollow used for rigging and place heavy equipment in the facility, usually made up in prefabricated blocks, are also considered in concrete in calculus.

Table 1.- Features of materials in MCNP6, adapted from [McConn *et al.*, 2011] and [Tesse *et al.*, 2018]*

Material	Composition (Atomic Fraction)	Density (g/cm^3)
Air	75.53% N, 23.18% O, 1.28 Ar, 0.01% C	$1.2 \cdot 10^{-3}$
Water	67% H, 33% O	1
Natural soil (Earth)	55% O, 23.8% Si, 11.10% Al, 4.20% Mg, 3.5% Fe, 1.7% H, 0.71% Ca	1.8
Air (void)	78% N, 22% O	$1.6 \cdot 10^{-11}$
Portland concrete	53% O, 33.7% Si, 4.4% Ca, 3.4% Al, 1.6% Na, 1.4% Fe, 1.3% K, 1% H, 0.2% Mg, 0.1% C	2.3
Low activation concrete*	47.8% O, 40.5% Ca, 8.9% C, 1.2% Si, 0.72% H, 0.27% Al, 0.24% Mg, 0.08% Na, 0.06% Fe, 0.03% K	2.18
Brass	58% Cu, 39% Zn, 3% Pb	8.4
Tungsten (Wolfram)	100% W74	19.3
Tin	100% Sn50	7.3
Iron	100% Fe56	7.87
Nickel	100% Ni58	8.9
Copper	100% Co63	8.96
Tantalum	100% Ta73	16.7
Beryllium	100% Be4	1.85
HD Graphite	100% C12	1.7
Aluminium	100% Al13	2.7

Regarding mechanical equipment, only those with yielding of secondary neutrons were modelled, mainly accelerator and beamline. S2C2 is a superconducting synchrocyclotron (RF frequency decrease with radius and also B for weak focusing), central magnetic field of 5.7 T, dee voltage of 11 kV, which produces 230 MeV monoenergetic protons, current up to 135 nA, with total weigh of 50 tons (41 in iron), diameter 2.5 m and height 1.59 m. The extraction system, efficiency near 50%, is type passive regenerative, works with pulses of 7 microsecond (repetition rate 1 KHz). The main elements of extraction are the pre-septum, septum and PMQ1/PMQ2 (permanent magnet quadrupoles), used to focus horizontally the beam when passing through the fringe field [Pearson *et al.*, 2013].

The beamline (BL) include the elements to drive the protons from the accelerator to the patient and could be divided into the energy selection system (ESS), in the accelerator room (AR), and the beam transport system (BTS), in the gantry room (GTR). The purpose of the ESS is to adapt the energy of protons (fixed in 230 MeV in PT cyclotrons) to the energy necessary in the treatment room, depending on the clinical requirements (minimum of 70 MeV). Since a large number of secondary neutrons are produced in the energy reduction process, the ESS is placed in the AR, as far from the patient as possible, with a shielding wall in between. The main elements of the ESS are quadrupoles, Q1C and Q2C, used to focus the beam extracted from the accelerator, the degrader (DEG), a rotating wheel with different materials and thicknesses that is moved to reduce the energy of the protons in the range 230 MeV to 70 MeV (range shifter), and finally the collimator (COL), a tantalum cylinder with a hole in the centre to focus and narrowing the beam again, after the collision in the degrader [Van de Walle *et al.*, 2018].

On the other hand, the beam transport system (BTS) are the elements from the exit of collimator until the nozzle in the GTR, where the suitable dose must be delivered to the tumor volume, using a pencil beam scanning (PBS) system. The PBS is integrated in the 30º inclined part of the gantry and achieves an accurate dose conformity. While the forward direction of the beam is controlled by the ESS, in lateral directions is deflected by scanning magnets (SM), placed before the final bending magnet of GTR (upstream scanning). This configuration accomplishes better SAD (source to gantry axis distance), a critical parameter in treatment quality. The typical features of treatment are dose rates of 2 Gy/l/min (10 nA), field sized in 20 x 24 cm^2, maximum range of 32 g/cm^2, range modulation in steps of 0.5 g/cm^2, and spot size at highest range under 3.5 cm. In PBS there are not compensator and collimator and the generation of secondary neutrons in the nozzle is negligible, whereas that efficiency is almost 100% [Nesteruk *et al.*, 2019].

There are different normal conducting magnetics accessories in the beam, as quadrupoles (Q), used to focus the beam along a specific direction, or dipoles, used for bending and change the direction of the beam, often called bends (B). Other no magnetics elements are collimators or slits (SL), used for controlling the spatial (divergence) and energetic extension (momentum), or beam profile monitors (BPM), used to ensure correct properties of the beam reaching to the patient. [Pearson *et. al.*, 2014]. As summary, Figure 2, shows the main electromechanical elements considered in the MCNP6 model.

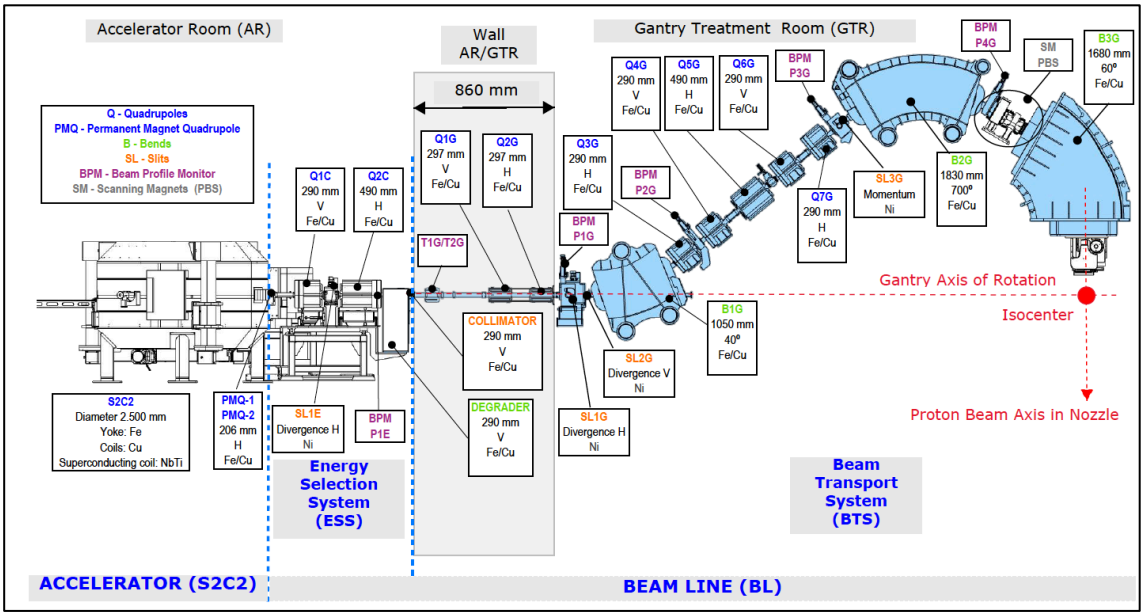

Figure 2.- CPTC Beamline main elements, adapted from [Hernalsteens *et al.*, 2018]

2.2.2. Beam losses and sources of radiation. Modelling all the components of the facility is neither viable nor useful from the point of view of the calculation radiation sources. The method followed is the point neutron-equivalent in which the radiation sources are the points where proton beam losses interacting with matter, considering a narrow beam perpendicularly to collision surface. These points are elements of facility where the protons change energy, direction or intensity.

In PT the clinical dose delivered is intended by monoenergetic beams at different energies, yielding Bragg peaks at different depths, depending on the target range to reach in tissue. This process is known as Spread-Out Bragg Peak (SOBP), and the different energies are achieved at the ESS [Gottschalk, 2018]. Following works in similar CPTC [Tesse, 2019], the energies considered to compound the SOBP in the model were 70 MeV (range of 4 g/cm^2 in water), 86 MeV, 116 MeV, 160 MeV, 200 MeV and 230 MeV (range of 32 g/cm^2 in water), and neutron sources were modelled with these assumptions.

2.2.2.1 Accelerator. Nominal extraction efficiency at 230 MeV is 50% [Pearson *et al.*, 2013], although an efficiency of 30% was assumed as a conservative approach, therefore 70% of produced protons are lost inside the cyclotron. In the source of protons energy is under 10 MeV and losses were assumed negligible. In agreement with literature [Urban and Kluson, 2012], 25% of losses were considered uniformly distributes along the

external radius of acceleration (iron), and the remaining 45% at the extraction system (septum and pre-septum in copper, and PMQ1/PMQ2 in iron and copper). There is a layer of 75 cm in iron all around the external acceleration radius and thus self-shielding inside of accelerator of yielded neutrons was assumed [Ferraro and Brizuela, 2015]. S2C2 was modelled as an electromagnetic pole cylinder (diameter 100 cm, copper), inside the magnet yoke cylinder (diameter 250 cm, iron), with 159 cm height.

2.2.2.2 Energy Selection System (ESS). Quadrupoles were modeled as hexagonal slabs of iron and copper, with lengths as shown in Figure 2. The published data of losses are 4.02% for Q1C and 14.01% for Q2C for all energies [Tesse, 2019]. The degrader (DEG) was modelled as a cylinder with an external diameter of 24 cm with different thickness depending on the energy at the exit. Beryllium was used up to 130 MeV (thickness of 19.137 cm for 70 MeV, 17.933 cm for 86 MeV and 15.196 cm for 116 MeV), graphite up to 220 MeV (thickness of 10.054 cm for 160 MeV and 4.599 cm for 200 MeV), and aluminium over 220 MeV (thickness 2.2 cm). In all cases the radius of the degrader was greater than the range of protons and the thickness is designed to achieve an energy at exit equal to the energy necessary in treatment room. Finally, the collimator (COL) was modelled as a cylinder of tantalum, with an external diameter of 6 cm, a thickness of 4 cm and a hole along its axis with 1 cm of diameter. Losses in divergence slits of ESS (SL1E) (placed between QC1 and QC2) were considered negligible in the model.

2.2.2.3 Beam transport system (BTS). Considering data of global efficiency, ε, namely, the fraction of protons extracted from the cyclotron that finally reach the phantom, estimated losses in BTS are within 5.67% at 70 MeV and 33.08% at 230 MeV [Tesse, 2019]. The main losses in BTS would be Q1G and Q2G (70-230 MeV, Fe/Cu), placed after the collimator, divergence slits, SL1G and SL2G (70-230 MeV, Ni), and energy/momentum slits (70-230 MeV, Ni). Using scanning methods, as PBS, an unimportant contribution of neutrons compared with former scattering methods is yielded [Hall, 2006]. Losses in other quadruples (Q3G, Q4G, Q5G, Q6G) bends (B1G, B2G, B3G) and beam profile monitors (P1G, P2G, P3G, P3G) were considered negligible.

2.2.2.4. Phantom (patient). In the model was considered a water phantom with a dimension of 40x40x40 cm^3 [Han et al., 2017], irradiated with a beam proton equal to the global efficiency at each energy, ε. Summary of losses in BL are collected in Figure 3.

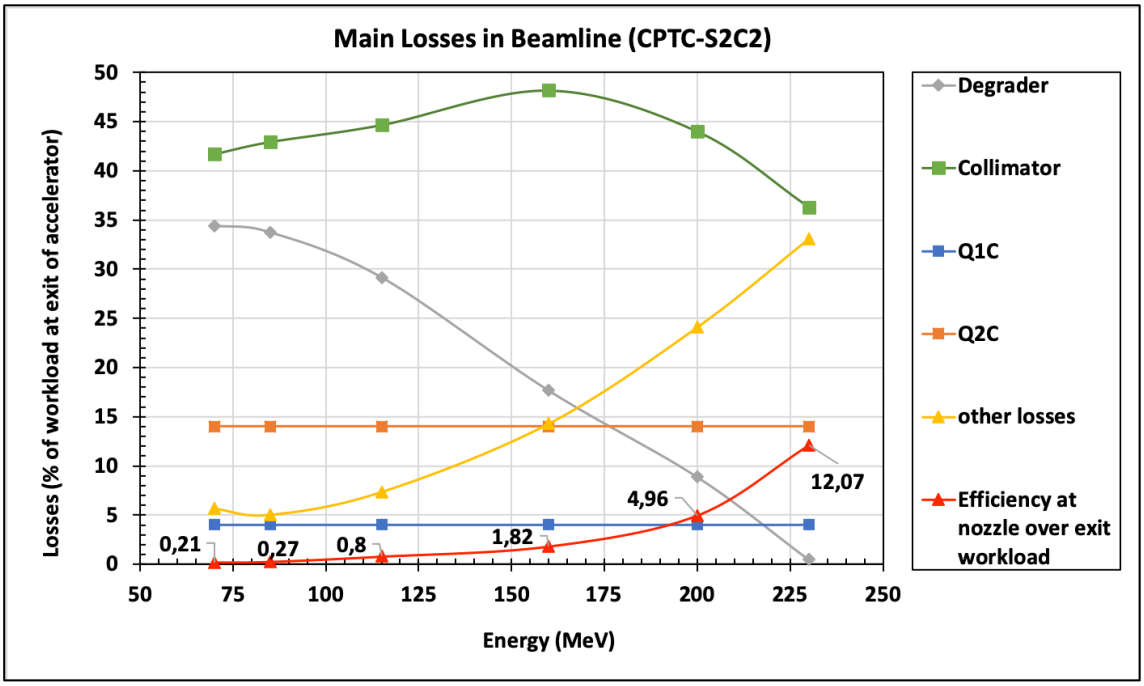

Figure 3.- Main losses in the beamline of CPTC, adapted from [Tesse, 2019]

2.2.3. Neutron production and physics models. Protons mainly interact with matter by inelastic scattering with electrons (dose in tumor), elastic or multi-coulomb scattering with nucleus (lateral penumbra), and direct nuclear interactions, spallation process, (SP), resulting in fields of charged particles, gamma-rays and neutrons, this last motivating the shielding in PTC. Classically two main stages are set in SP, intranuclear cascade (INC), a chain reaction induced by high energy protons, above 20 MeV, inside the nucleus, with large energy transferred to few particles and forward peaked emission, and secondly, the evaporation process (EVP), protons under 20 MeV, where nucleons and radiation are emitted isotropically. The SP finish with activation and decay reactions [Gottschalk, 2018]. Neutrons yielded, with spectra from zero until the energy of the impinging protons, strongly depends on the energy of these, the angle and the material of collision. The high energy neutrons generated produce new INC, EVP and activation process, mainly inelastic scattering (10 MeV to 50 MeV), elastic scattering (energy under 10 MeV), and finally capture and activation [Lai *et al.*, 2015].

In MCNP6 there are different physical models to simulate the spallation process and the neutron production, however, the models chosen were the default values, the Bertini model (INC) followed by the Dresner model (EVP), because with those models the computation time is shorter and the results achieved are more conservative [Solc, 2019].

Following the point neutron-equivalent model (points where protons produce neutrons), and to define the main parameters of source-term, as intensity, energy and angle [Urban and Kluson, 2012], several simulations were carried out, reaching the neutrons yielded, through a condensation process, in the collision of protons with different materials, angles and energies. Further data, experimental and simulated, can be found elsewhere [Matsuda *et al.*, 2008], [Tsai *et al.*, 2018].

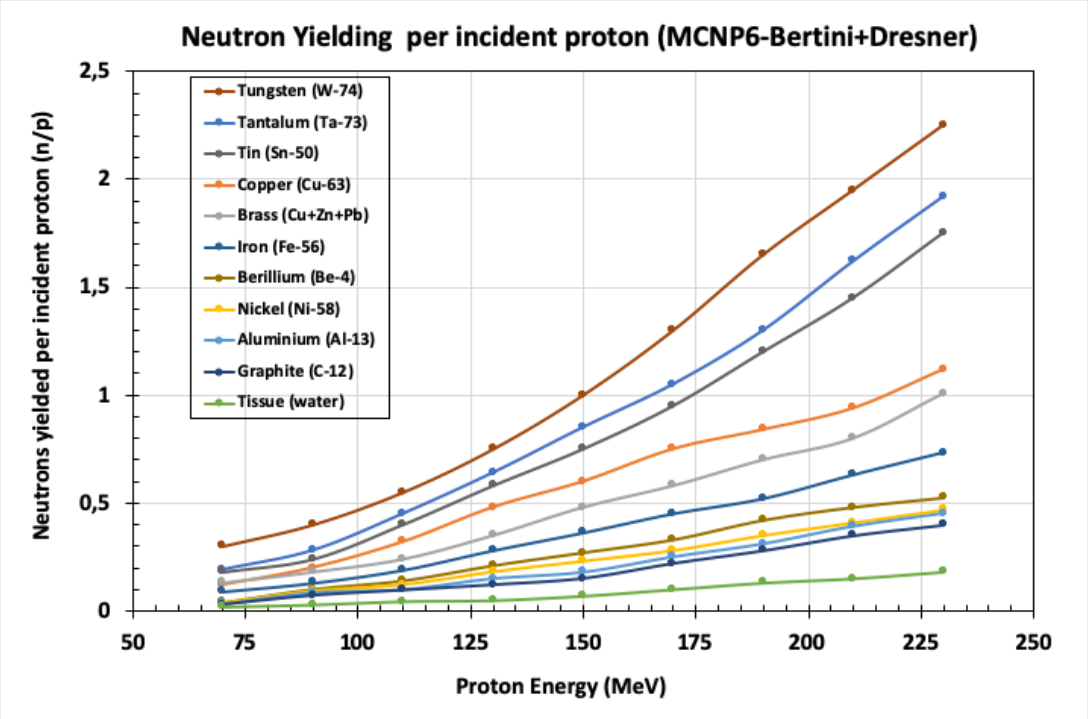

Figure 4.- MCNP6 neutron yield per proton

2.2.4. Facility Workload. The workload was estimated in agreement with published data for these CPTC, in nA·h per year in each energy, at the exit of accelerator [Tesse, 2019], assuming a conservative approach of 16-hour workday in two 8-hour shifts, six working days per week, and fifty weeks per year, 450 patients/year, 17.000 sessions, with 2 Gy/session, considering the clinical data about number of patients and typical treatment plans [Verma *et al.*, 2016]. Occupancy factors were obtained from international recommendations by choosing the most conservative options [IAEA, 2006].

Final assumptions were that the beam work a 25% with gantry oriented to the floor, 25% oriented to the ceiling, and 50% oriented to south wall, however just ceiling and south wall orientations were considered. Workload and data used are collected in Table 2.

Table 2.- Workload, losses, efficiency and main parameters of beamline in S2C2

Nominal Energy (MeV)	Nominal Range (g/cm^2)	Current per nA (p/s)	Workload (nA·h)/y (phantom)	Efficiency at Nozzle (%)	Q1C losses (%)	Q2C losses (%)	DEG losses (%)	COL losses (%)	Other losses (%)
70	4.1	$3.8 \cdot 10^6$	65.6	0.21	4.02	14.01	34.4	41.69	5.67
86	5.9	$8.3 \cdot 10^6$	74.056	0.27	4.02	14.01	33.73	42.93	5.04
116	10.1	$2.5 \cdot 10^7$	89.911	0.8	4.02	14.01	29.16	44.66	7.35
160	17.6	$5.6 \cdot 10^7$	113.65	1.82	4.02	14.01	17.67	48.19	14.29
200	26.0	$1.3 \cdot 10^8$	128.53	4.96	4.02	14.01	8.88	44.02	24.11
230	32.9	$2.5 \cdot 10^8$	145.48	12.07	4.02	14.01	0.5	36.32	33.08

2.2.5. – Area monitoring magnitude. In agreement with ICRU/ICRP, the operational quantity chosen to assess the shielding was the ambient dose equivalent, H*(10), along the enclosures of a standard CPTC, because is a conservative magnitude [ICRP, 1996]. H*(10) was obtained through the convolution of neutron fluence, $\Phi(E)$, cm^{-2}, and the ICRU fluence to ambient dose equivalent conversion function, h(E), $Sv \cdot cm^2$ [Gallego *et al.* 2004], and its expansion up to 240 MeV [Sannikov and Savitskaya, 1997].

2.2.5. MCNP6 settings and calculations. The shielding verification was carried out by estimating the ambient dose equivalent at different the points of interest behind the main enclosures. ENDF, evaluated nuclear data libraries, La150n library, were used up to 150 MeV [Conlin, 2014], and nuclear models above that energy, the Bertini Model for INC reactions, and Dresner Model for EVM. When the isotope was not available in the library, the ENDF-B.VII was used up to 20 MeV, and above that energy the nuclear model indicated above. The number of stories carried out was 10^9, to achieve an uncertainty under 3%, considering 20 energy groups (from 10^{-9} MeV to 230 MeV), in agreement with the ICRP functions, and using $S(\alpha,\beta)$ model reactions with polyethylene.

The origin of coordinates is in the lower left corner in the layout (external corner of west and south walls), and the zero-height corresponding to the floor of the AR. As variance reduction in cells of the walls, roof and air in vaults, biasing methods and weight factors were used based on geometry splitting and Russian roulette. All rooms were considered air-filled and void in the proton beam. The results were computed using superposed mesh tallies inside the facility, along the walls and roofs and outside the enclosures (each 20 cm in wall sections and each 50 cm along the length).

Two different models were developed in this work, with the goal of verify the shielding in the CPTC defined above. On the one hand, in Model 1, the most conservative hypothesis for commissioning were assumed. The material chosen in enclosures was regular Portland concrete, density 2.3 g/cm^3, and four main sources of radiation were considered: 1) Accelerator: 25% losses in circumference (Fe/Cu) and 45% losses at the extraction (Fe/Cu); 2) ESS: 18.03% in Q2C for all energies; no losses in Q1C; losses in degrader and collimator following Table 2; 3) BTS, considering 60% of other losses in Q2G and 40% in SL1G and SL2G; 4) Phantom, efficiency following Table 2.

On the other hand, in Model 2, more realistic but still quite conservative hypothesis were assumed. In this model, the material chosen in enclosures was low activation concrete, density 2.18 g/cm^3, and also four main sources of radiation were considered, but with some changes: 1) Accelerator: Same assumptions as model 1; 2) ESS: losses following Table 2; 3) BTS, considering 10% of other losses in Q1G, 50% in Q2G, 35% in SL1G and SL2G and 5% in SL3G; 4) Phantom: As model 1.

The model of the CPTC developed in MCNP6 is shown in Figure 5, including the elevation (left-up), footprint (left-down) and 3D view (right), with the designations of different enclosures as indicated in results.

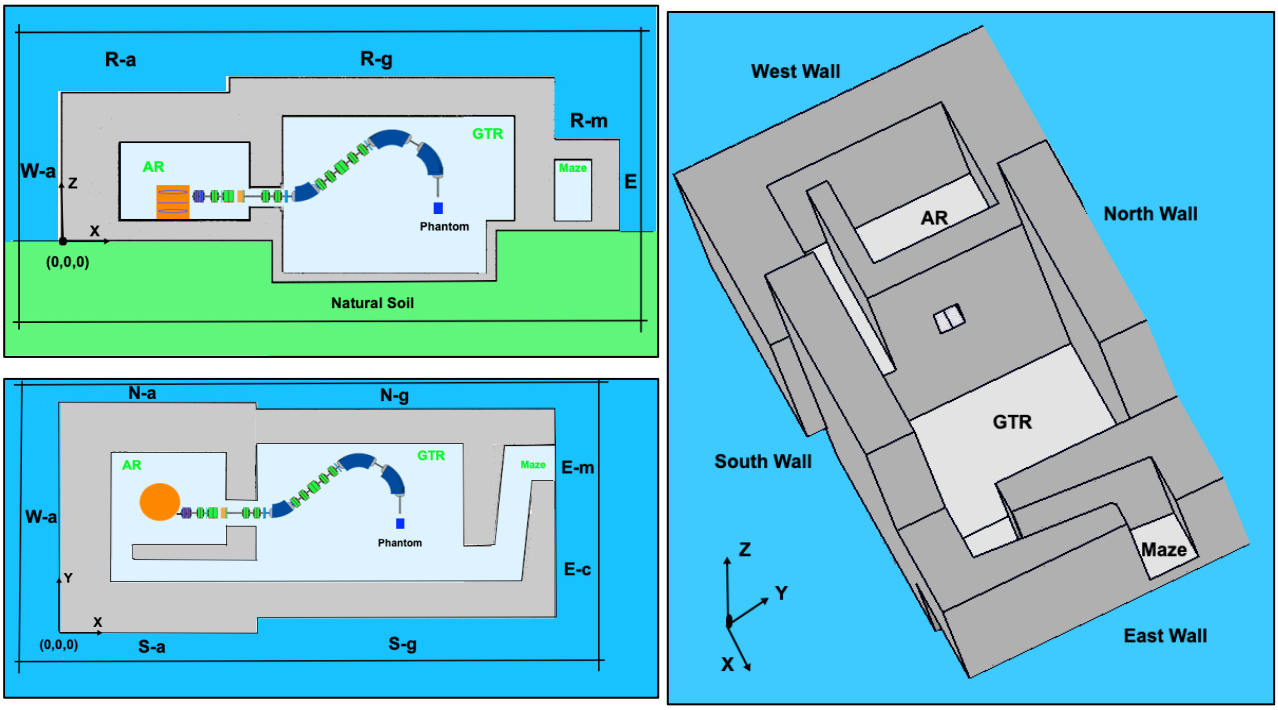

Figure 5.- CPTC model in MCNP6

3. – RESULTS AND DISCUSSION

3.1. – Ambient Equivalent Dose around the facility

Only the dose from neutrons was considered, since the dose per photons is an order of magnitude lower, and in the verification phase of the shielding it is not relevant. Alike, at this stage of commissioning, the dose coming from potential activated elements was not considered in the results neither.

3.1.1. Enclosures. The values of H *(10) behind the walls are collected in Figures 6 to 10, including the four different sources considered in the calculation: accelerator (purple), ESS (orange), BTS (grey) and phantom (green). The final sum of the four sources is reflected in the blue line for model 1, conservative. In model 2, however, the lines corresponding to each of the sources are not included for clarity, and only the total sum of the sources is included, corresponding to red line in graphs. Orientation and projection of the different walls are represented in the figures by gray rectangles.

As shown in Figure 6, the south wall (SW), has been divided into the accelerator zone, S-a, and the area of the treatment room, S-g, indicated at the bottom of the graph.

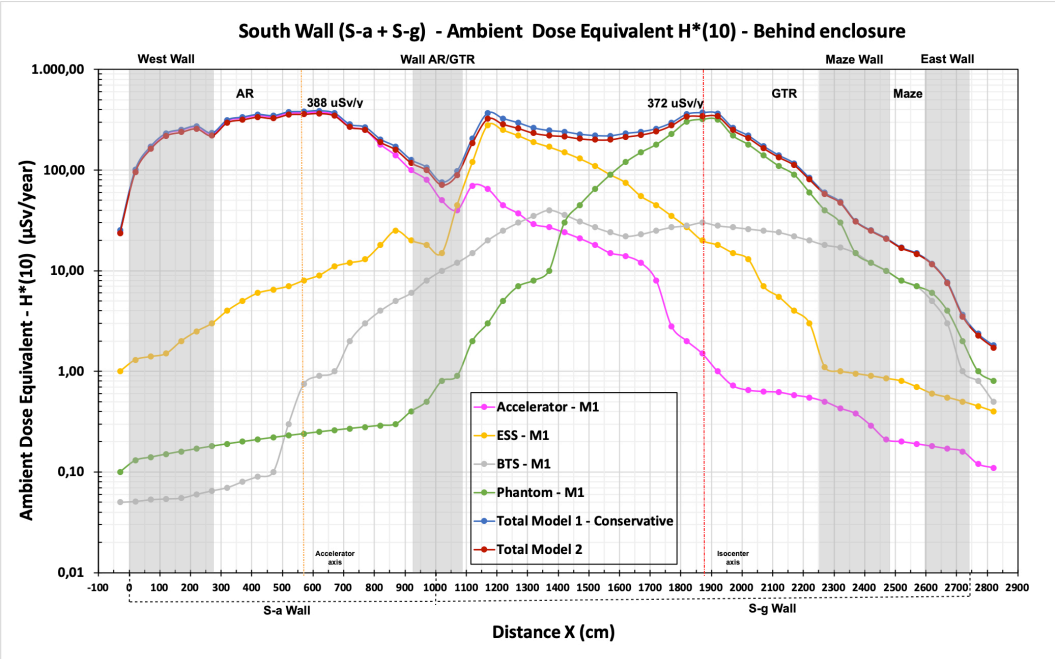

Figure 6.- MCNP6 shielding verification in South Wall (S-a and S-g)

The highest doses outside the SW are obtained in the area of both the cyclotron X-axis (x_a = 570 cm) and the isocenter X-axis (x_i = 1875 cm). In S-a wall, the high dose is 388 µSv/year (x = 620 cm), and in the S-g part 372 µSv/year (x = 1870 cm), with a gantry orientation of 90º (pointing to SW). These are points where a lot of higher energetic neutrons are coming from the external circumference of accelerator and the phantom/patient. The high dose is mainly due to the neutron peak in the 100 MeV originated in the INC. There is a third high value of 388 µSv/year, near the wall AR/GTR, x = 1170 cm, produced by the ESS. The BTS generate a moderated dose of 40 µSv/year, in the GTR. Nonetheless, H*(10) behind the SW is always less than 50% of the legal limit, even with the more conservative options.

The east wall (EW) has been divided into the area of CTR (control treatment room), called E-c, and the zone of the entrance to the maze, indicated as E-m, as shown at the bottom of Figure 7, with cyclotron Y-axis is in y_a = 715 cm and isocenter Y-axis in y_i = 660 cm.

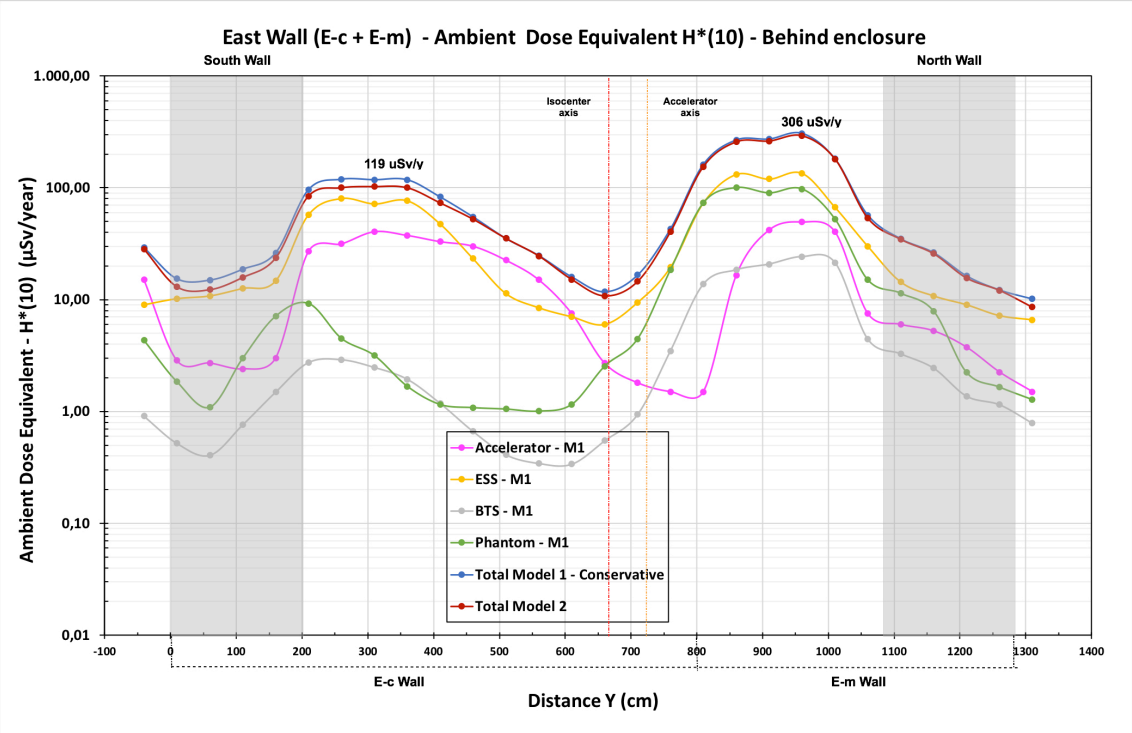

Figure 7.- MCNP6 shielding verification in East Wall (E-c and E-m)

The highest dose at the EW was reached in the entrance to the maze (y = 960 cm), in E-m part, with a value of 306 µSv/year, because in that area there is only one leg of the maze. In the E-c part, the dose is almost a third, 119 µSv/year, in the TCR (y = 260 cm).

Regarding north wall (NW), with H*(10) collected in Figure 8, as the south wall (SW) has been divided into two main parts, the accelerator zone, N-a, and the area of the treatment room and gantry, N-g, indicated at the bottom of the figure.

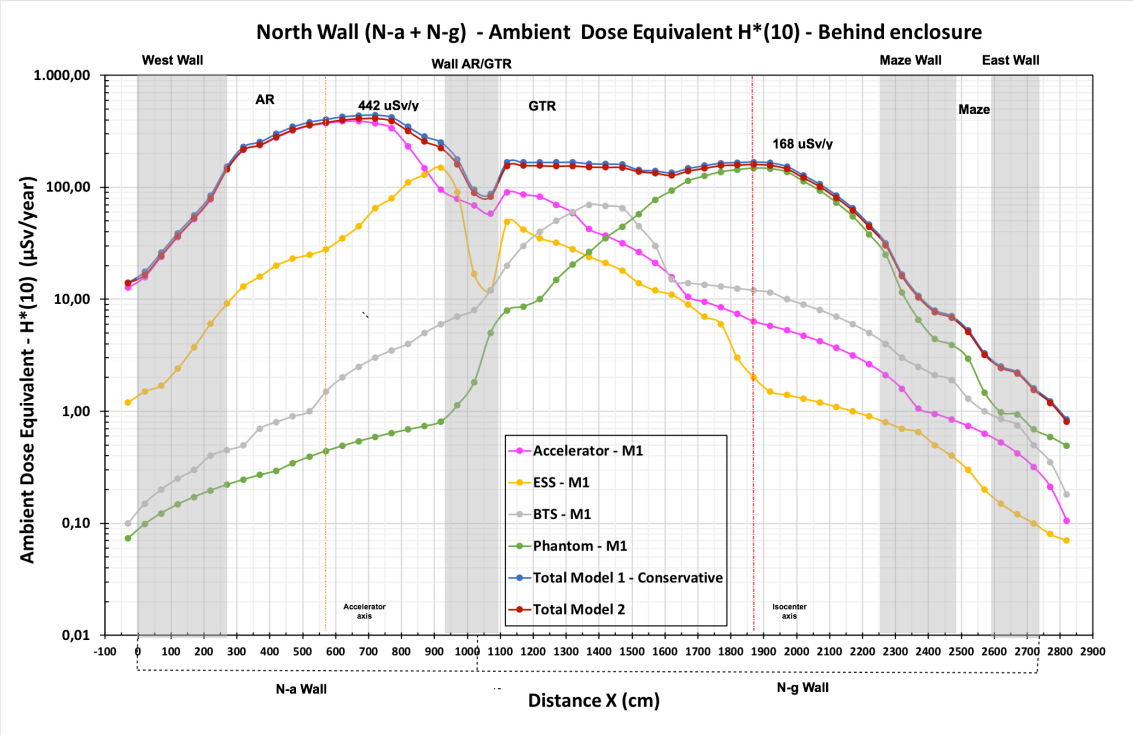

Figure 8.- MCNP6 shielding verification in North Wall (N-a and N-g)

In N-a, the maximum dose, 442 µSv/year (x = 720 cm), is highest than S-a, due to the absence of the wall of maze, and come mainly from the sum-up of accelerator and ESS sources. In N-g the high level of dose is also near the isocenter zone, with a value of 168 µSv/year (x = 1820 cm), coming from the phantom. This value is half of S-g part because the gantry rotated fixed in the SW, so never could point to NW, while when the gantry has an orientation of 90º is pointing directly to the SW.

On the other hand, the dose near the wall between both rooms, AR/GTR, is 164 µSv/year, very close to the dose at the isocenter, due to the sum-up of phantom and ESS sources. In this area there is an important contribution coming from the BTS source, with almost 70 µSv/year, mainly due to the neutrons generated in the divergence slits (SL1G) and the quadrupoles located in the passage of the wall Q1G and Q2G). Nonetheless, as SW, the ambient equivalent dose behind the NW is always less than 50% of the legal limit either, even with the conservative options.

The west wall (WW) only have one part corresponding to the accelerator, indicated as W-a, as shown in Figure 9. Results of WW show a highest dose level of 455 µSv/year in y = 610 cm, near to the isocenter Y-axis (y = 660 cm), coming mainly from the sum-up of accelerator and ESS sources. In this part, the radiation coming from BTS or phantom sources is negligible due to the wall between AR and GTR.

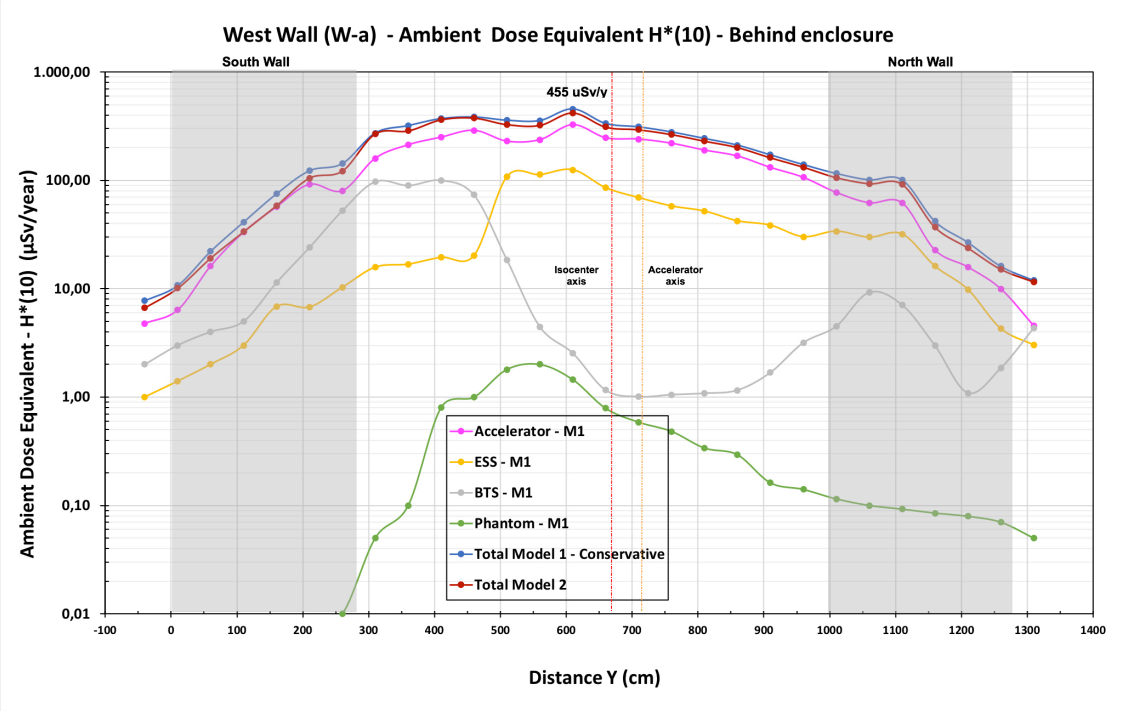

Figure 9.- MCNP6 shielding verification in West Wall (W-a)

The final main enclosure, the roof, has been divided into the area of accelerator (R-a), gantry treatment room (R-g) and maze (R-m), as shown at the bottom of Figure 10, including in the figure just results of R-a and R-g zones.

The highest dose was reached at the roof in x = 870 cm, 439 µSv/year (x = 720 cm), in the R-a area, and coming in first place from the ESS source and secondly from the accelerator. In R-g the high level of dose is near x = 1120 cm, with a value of 264 µSv/year, coming from the phantom. The dose reached in the R-m is 404 µSv/year, behind x = 2225 cm, no shown in the figure. The main reason of the high dose in this part is that in the standard CPTC modelled was considered a R-m roof with a thickness of just one meter, assuming that the superior area will be without use and people above. In the real CPTC, the thickness of this roof must be adapted according to the final use overhead.

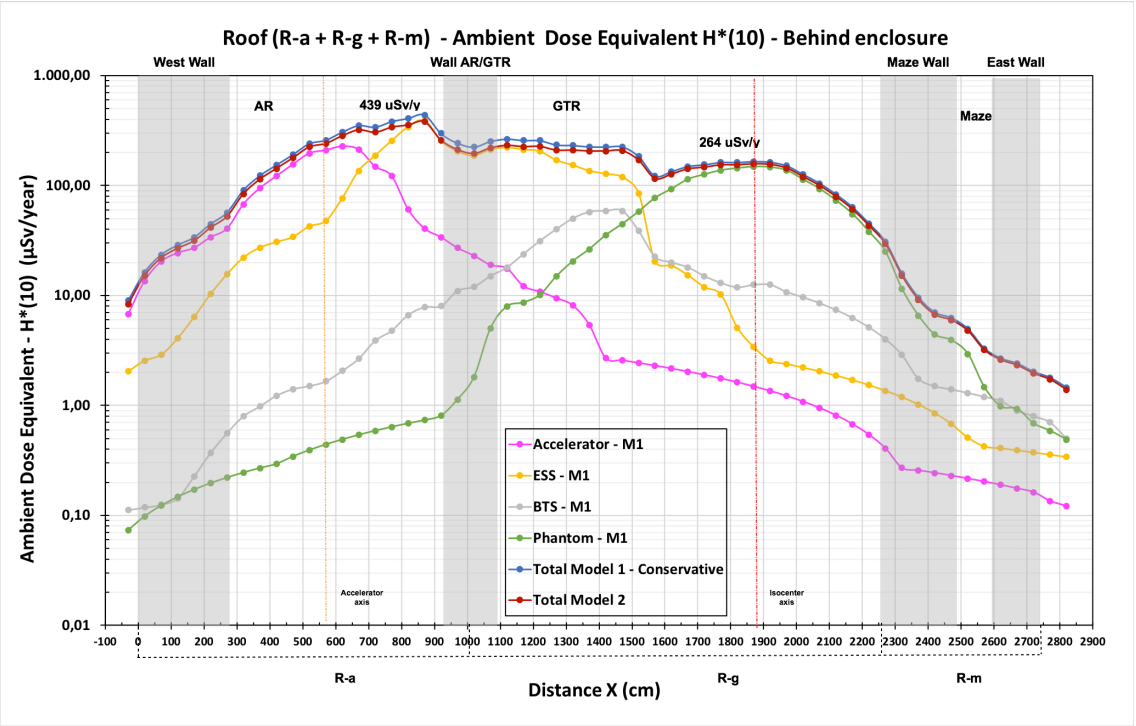

Figure 10.- MCNP6 shielding verification in Roof Enclosures (R-a, R-g and R-m)

3.1.2. Attenuation in depth. The length of attenuation and dose in depth is shown in Figure 11, corresponding to enclosures W-a and N-a around the accelerator room (AR), where the highest dose values were reached, both with a thickness of 280 cm. For Model 1, W-a is in blue and N-a in orange, while for Model 2, W-a is in grey and N-a in red.

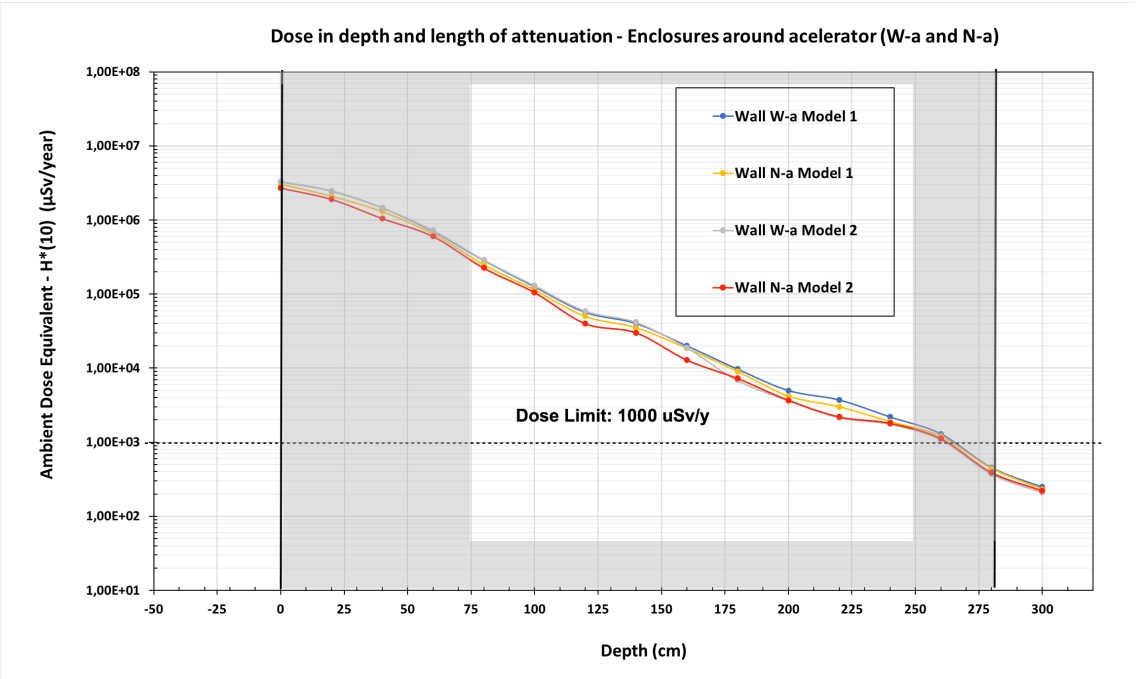

Figure 11.- MCNP6 attenuation length and dose in depth of enclosures W-a and N-a

As can be seen in the graph, the attenuation curve and depth dose corresponding to the walls surrounding the accelerator are very similar regardless of the wall and type of concrete used. This type of material has more influence on activation, whose study is not included in this work, rather than attenuation. Approximately every meter of depth the maximum dose is reduced by an order of magnitude.

The dose below the legal limit (1000 µSv/year) is reached close to the depth of 260 cm, hence, even with the most conservative assumptions, there is an additional thickness of 20 cm in all enclosures, which is equivalent to 7% of the wall or ceiling.

3.1.3. Dose map. The graph with the isodose curves obtained with the assumptions corresponding to the conservative sources of Model and regular Portland concrete is shown in Figure 12, with grey color designating the legal dose limit, that is achieved inside all the enclosures. Orange colors show dose under those limit values.

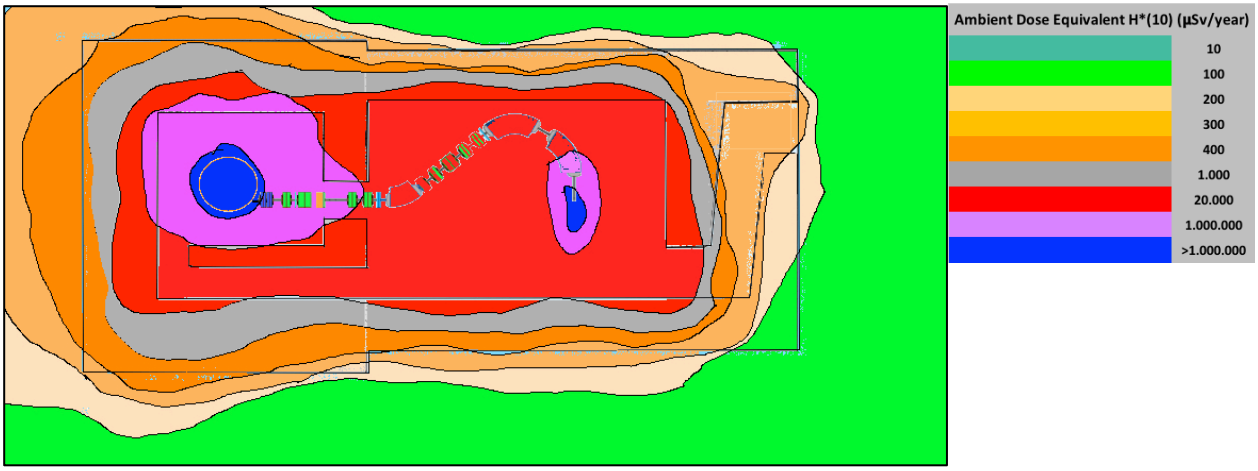

Figure 12.- MCNP6 dose map

3.2. – Benchmark of radiation source models and materials

The final benchmarking of results reached in each enclosure with both models are shown in Figure 13, where blue bars corresponding with conservative Model 1 and red bars with Model 2. The highest dose values are achieved with the Model 1, in the enclosures around the accelerator, the west wall, zone W-a, with a value of 455 µSv/year, the north wall , zone N-a, with a value of 442 µSv/year, and finally the roof, zone R-a, with a value of 439 µSv/year.

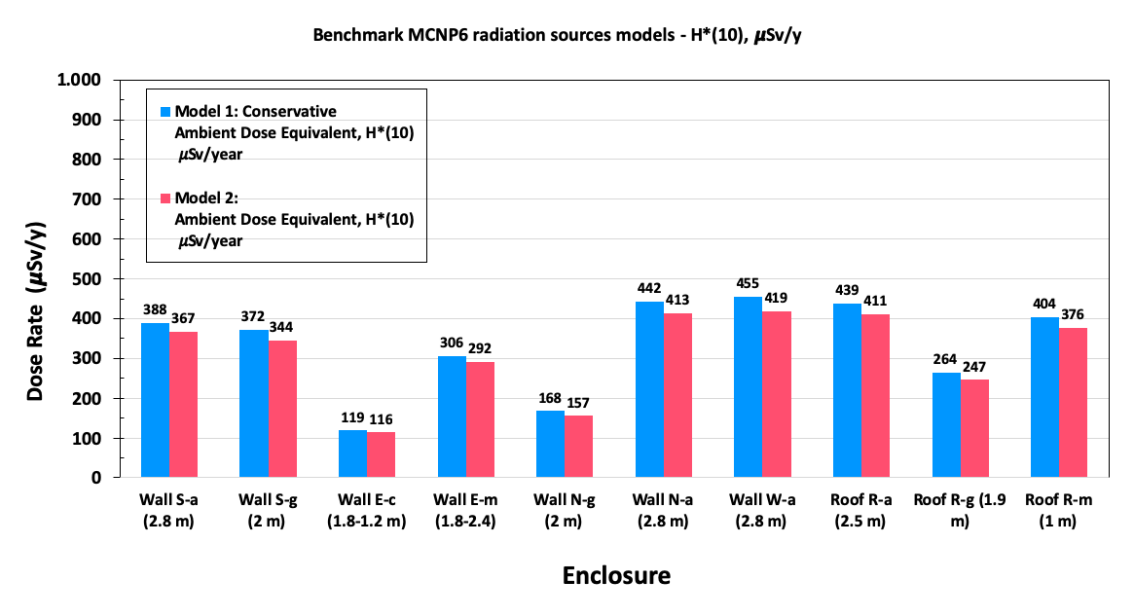

Figure 13.- MCNP6 shielding verification: Benchmark of sources models

With more realistic assumptions of beam losses and sources chosen in Model 2 the results reached are between 10% and 15% below the base Model 1. In any case the results are under the legal requirements of 1 mSv/year, even with the most conservative assumptions, the results do not reach half of dose limits.

There are different uncertainties that must be reduced in the stage of building and final definition of enclosures, mainly the characteristics of the concrete finally employed, that is, the percentage of Hydrogen, that could vary from a minimum of 0.4% to 2.1%, depending of the country and the supplier, and final density, that could vary from 2.1 to 2.4 g/cm^3. These two parameters are critical and have a high impact in the attenuation and shielding and should have been collected along the build of the center. Another sources of uncertainty are the physics models and nuclear data library used in the calculus, varying from 1.3 to 1.9, therefore a benchmarking with other CPTC and experimental measurements should be carried out further.

The main problem is what could be called the *density of the radiation*, dose per square meter, which is higher in CPTC than in MPTC, mainly because the footprint is smaller and the distances shorter. This higher concentration of the radiation fields could lead to greater activation of the shielding materials, and therefore the most suitable materials are those of low activation rather than high density.

4. - CONCLUSIONS

The effectiveness of the shielding against stray neutron radiation in a CPTC has been verified for the building commissioning of a center similar to that planned for 2019 in Spain. The CPTC model has been developed in the Monte Carlo code MCNP6.2 based on the basic architectural plans, using CAD designs and installation meshing systems. Different assumptions have been simulated, depending on the working conditions considered, the sources of radiation produced, and the physical models of proton-matter interaction, based on the more conservative base hypothesis, to continue with models that incorporate new data and more realistic assumptions based on recent publications and simulate different building materials against neutron radiation. The operational quantity used in the assessment of the shielding was the conservative magnitude ambient equivalent dose, H*(10), outside the enclosures of a standard CPTC.

Using the assumptions most conservative, the highest dose values are reached in the enclosures around the accelerator room (AR), specifically the west wall (W-a), 455 μSv/year, the north wall (N-a), 442 μSv/year, and the roof (R-a), 439 μSv/year. The main radiation sources coming from accelerator and phantom, with an important contribution also from the ESS and in some cases (NW) from the BTS. For optimized models, based on more realistic assumptions and precise, Model 2, the results are between 10% and 15% below. In any case the results are under the legal requirements of 1 mSv/year, even with the most conservative assumptions, the results do not reach half of dose limits. The main problem in the CPTC is the radiation density that causes a greater activation of the shielding materials and therefore it is more advisable to use low activation materials

There are different sources of uncertainty in the model, mainly the concrete final composition and density, nuclear models and data, therefore, results will be compared with experimental measurements during commissioning of the center. For this purpose, the response of REM-meter type extended range detectors was characterized in previous work within the research project. Experimental measurements will allow contrasting the different models developed in this work and to develop a methodology for analyzing the efficacy against neutrons in CPTC, evaluating the dose for workers and the general public.

Acknowledgments and Funding

Gonzalo F. Garcia-Fernandez has developed this work under the Industrial Doctorate Program, IND2017/AMB-7797, *Contributions to Shielding and Dosimetry of Neutrons in CPTC*, funded by Madrid Autonomous Region (CM), in accordance with the agreement between the Universidad Politecnica de Madrid (UPM) and the company Biología y Técnica de la Radiacion, S.L. (Bioterra, S.L.).

Lenin E. Cevallos-Robalino, thanks to Secretaria Nacional de Educación Superior Ciencia y Tecnología of Ecuador (SENESCYT), for the scholarship to carry out postgraduate studies in Madrid, Spain.

Roberto García-Baonza thanks the Chair of Nuclear Safety “Federico Goded” between the Nuclear Safety Council (CSN) of Spain and Universidad Politecnica de Madrid (UPM) for the grant received (No. SN1805410112).

REFERENCES

Agosteo, S., et al., 1998. Secondary neutron and photon dose in proton therapy. Radiotherapy and Oncology **(48)**: 293–305.

Avery, S. et al., 2008. Analitical shielding calculations for a proton therapy facility. Radiation Protection Dosimetry **(131), 2**: 167-179.

Conlin, J.L., 2014. *Listing of Available ACE Data Tables*. LA-UR-13-21822, LANL, Rev. 4.

Ferraro, D., Brizuela, M., 2015. Tests & benchmarking methodology for a 230 MeV proton accelerator calculations. Conference proceedings. Asociación Argentina de Tecnología Nuclear, XLLI Reunión Anual.

Gallego, E., Lorente, A. and Vega-Carrillo, H.R.,2004. Characteristics of the neutron fields of the facility at DIN-UPM. Radiation Protection Dosimetry **110**:73-79.

García-Fernández, G.F., Gallego, E. and Nuñez, L., 2019. The new protontherapy centers in Spain (Los nuevos Centros de Protonterapia en España)). Radioprotección. Publication SEPR, 94, March: 19-28.

Gottshalks, B. Radiotherapy proton interactions in matter. Chapter 2 in: Proton Therapy Physics, 2nd edition, H. Paganetti ed., Taylor & Francis (2018).

Hall, E.J., 2006. Intensity-modulated radiation therapy, protons, and the risk of second cancers. International journal of radiation oncology, biology, physics **(65)**: 1-7.

Han, S-E, Cho, G. and Lee, S.B., 2017, An Assessment of the Secondary Neutron Dose in the Passive Scattering Proton Beam Facility of the National Cancer Center. Nuclear Engineering and Technology **(49):** 801-809.

Hernalsteens, C. et al., 2018. Seamless beam and radiation transport simulations of IBA Proteus Systems using BDSIM. 13th Int. Computational Acc. Physics Conf. ICAP2018, Jey West, FL, USA.

Hitachi, 2019. Proton Beam System Brochure and Technical Inf. Online. July 2019.

IAEA, 1998. Radiological Safety Aspects of the Operation of Proton Accelerators. International Atomic Energy Agency, **Technical Reports 283**, Vienna.

IAEA, 2006. Radiation Protection in the Design of Radiotherapy Facilities. International Atomic Energy Agency, **Safety Reports Series 47**, Vienna.

IBA, 2019. ProteusONE Brochure and Technical Information. Online. July 2019.

ICRP, 1996. Conversion coefficients for use in radiological protection against external radiation. Annals of the ICRP Vol. 26, 3/4, ICRP **Publication 74**.

Ipe, N.E., 2010. Shielding Design and Radiation Safety of Charged Particle Therapy Facilities. PTCOG **Report 1**, Particle Therapy Cooperative Group.

Jägerhofer, L. et al., 2017. A shielding concept for the MedAustron facility. In: EPJ Web Conference 153, p. 04006.

Lai, BL., Sheu., RJ and Lin, UT., 2015. Shielding analysis of proton therapy accelerators: a demonstration using Monte Carlo-generated source terms and attenuation lengths. Health Phys **108(2 Suppl 2)**:S84-93.

Makita, Y. et al., 2004. Radiation shielding design of a cancer therapy facility using compact proton sybchrotron. J. of Nuclear Science and Tech., **Supp. 4**: 18-21.

Matsuda, N., et al., 2008. Analyses of Benchmark Problems for the Shielding Design of High Intensity Proton Facilities. Safety Div. of J-PARC Center-JAEA Technology.

McConn R. et al., 2011 Compendium of Material Composition Data for Radiation Transport Modeling. PNNL-15870 Revision 1. US DHS and US DoE.

Mohan, R. and Grosshans, D., 2017. Proton therapy - Present and future. Advanced drug delivery reviews,**109**, 26–44.

NCRP, 2005. Radiation Protection for Particle Acceleration Facilities. Recommendations of the National Council on Radiation Protection and Measurements, **Report 144**, Revision. NCRP.

Nesteruk, K.P. et al., 2019. Large energy acceptance gantry for proton therapy utilizing superconducting technology, Physics in Medicine & Biology, sub. January 2019.

Owen, H., Lomax, A. and Jolly, S., 2016. Current and future accelerator technologies for charged particle therapy. Nuc. Inst. and Methods in Physics R. **A (809)**: 96-104.

Pearson, E. et al., 2013. The new IBA superconducting synchrocyclotron (S2C2): From modelling to reality. 11th Int. Meeting on Nuclear Ap. of Acc., Bruges, Belgium.

Pearson, E. et al., 2014. Magnet developments and commissioning for the IBA compact gantry. IEEE Transactions on Applied Superconductivity **(24)**.

PTCOG, 2019. Particle Therapy Facilities. Reviewed July 2019.

Prusator, T., Ahmad, S. and Chen, Y., 2017. Shielding verification and neutron dose evaluation of the Mevion S250 proton therapy unit. Journal of Applied Clinical Medical Physics **(19-2)**: 305-310.

Sannikov, A.V, Savitskaya, E.N., 1997. Ambient dose equivalent conversion factors for high energy neutrons based on the ICRP 60 recommendations, Radiation protection dosimetry **70**: 383-386.

Schneider, U., Hälg, R.A. and Lomax, A., 2017. Neutrons in active proton therapy: Parameterization of dose and dose equivalent. J. Medical Physics **(27)**: 113-123.

Solc, J., 2019. Comparison of proton interaction physics models and cross section libraries for proton therapy Monte Carlo simulations by MCNP6.2 code. Radiation Measurements, **125**: 57-68.

Stichelbaut, F. Closset, M and Jongen, Y., 2014. Secondary Neutron Doses in a Compact Proton Therapy System. Radiation Protection Dosimetry **16**1, 1-4: 368–37.

Tesse, R. et al. GEANT4 benchmark with MCNPX and PHITS for Activation of Concrete. Nuclear Inst. and Methods in Physics Research B **(416)** 2018; 68-72.

Tesse, Robin. 2019. Quantitative methods to evaluate the radioprotection and shielding activation impacts of industrial and medical applications using particle accelerators. ULB-EPB.

Urban, T. and Kluson, J., 2012. Shielding calculation for the Proton-Therapy-Center in Prague, Czech Republic. Radioprotection **(4):** 583-597.

Van de Walle, J., et al., 2018. Beam dynamics simulations of medical cyclotrons and beam transfer lines at IBA. 13th Int. Computational Acc. Physics Conf. ICAP2018, Jey West, FL, USA.

Verma, et al., 2016. Cost-comparativeness of proton versus photon therapy. Progress in Nuclear Science and Technology.

Werner, ChJ., 2017. MCNP® User's Manual, Code Version 6.2. Los Alamos National Laboratory LA-UR-17-29981.

Werner, ChJ. et al., 2018. MCNP® Version 6.2 Release Notes. Los Alamos National Laboratory LA-UR-18-20808.